

# A Critical Examination of Halo White Dwarf Candidates

P. Bergeron

*Département de Physique, Université de Montréal, C.P. 6128, Succ. Centre-Ville,  
Montréal, Québec, Canada, H3C 3J7.*

bergeron@astro.umontreal.ca

## ABSTRACT

A detailed analysis of halo white dwarf candidates is presented, which is based on model atmosphere fits to observed energy distributions built from photoelectric or photographic magnitudes. Most of the candidates identified in reduced proper motion diagrams are shown to be too warm ( $T_{\text{eff}} > 5000$  K) and most likely too young to be members of the galactic halo, while the tangential velocities of the cooler and thus older white dwarfs are shown to be entirely consistent with the disk population. The results suggest that some white dwarf stars born in the young disk may have high velocities with respect to the local standard of rest. Such objects could represent the remnants of donor stars from close mass-transfer binaries that produced type Ia supernovae via the single degenerate channel, or other scenarios suggested in the literature. Ongoing surveys that rely solely on reduced proper motion diagrams are likely to identify more of these high velocity young degenerates, rather than to unveil the old white dwarf population of the galactic halo. The importance of infrared photometry for studying extremely cool white dwarfs is also emphasized.

*Subject headings:* Galaxy:halo, stars:kinematics, white dwarfs

## 1. Introduction

The first white dwarf stars to have formed in the galactic halo are expected to be extremely old ( $\tau > 14$  Gyr), cool ( $T_{\text{eff}} < 4000$  K), and have low luminosities ( $L/L_{\odot} < 10^{-5}$ ). They should also have large proper motions as a result of their high velocities with respect to the local standard of rest. The latter defines the frame of reference near the sun that rotates about the center of the Galaxy with a velocity of  $\sim 220$  km s $^{-1}$ . Moreover, if these white dwarfs have hydrogen-rich atmospheres, the collision-induced absorptions by molecular hydrogen would make these objects appear bluish in color-magnitude diagrams (see, e.g.,

Hansen 1998). These combined characteristics have led several investigators to look for this halo population of large proper motion white dwarfs by using digitized photographic plates taken at various epochs, and in particular by studying the location of individual stars in the so-called reduced proper motion diagrams. The identification of this halo population will help to estimate the contribution of white dwarf stars to the mass budget of the galactic halo, and determine whether they could account for the reported microlensing events.

The direct detection of galactic halo dark matter has been claimed by Oppenheimer et al. (2001, hereafter OHDHS) who identified 38 cool halo white dwarf candidates in the SuperCOSMOS Sky Survey, with an inferred space density that could account for 2% of the halo dark matter. This conclusion, however, has been challenged repeatedly since then by several authors (see Torres et al. 2002, and references therein). While some studies have reinterpreted the white dwarf kinematics (Reid et al. 2001), others deal with a reevaluation of the distances and tangential velocities (Torres et al. 2002) or age distribution (Hansen 2001).

In this paper, we take another look at halo white dwarf candidates reported in the literature. Our approach differs from previous investigations, however, in that we go back to the original published magnitudes – photoelectric or photographic, and attempt to extract the fundamental stellar parameters using model atmosphere fitting techniques that were developed to study the cool white dwarfs in the galactic disk. We first analyze halo white dwarf candidates with published trigonometric parallax measurements for which stellar masses and cooling ages can be determined. Then we reexamine the sample of white dwarfs reported by OHDHS using a similar approach.

## 2. White Dwarfs with Trigonometric Parallax Measurements

Liebert et al. (1989) were the first to identify white dwarfs in the solar neighborhood that could be interpreted as interlopers from the halo population of the Galaxy. Their Figure 2 shows the distribution of tangential velocities ( $v_{\text{tan}}$ ) with  $M_V$  for the sample used by Liebert et al. (1988) to measure the cool white dwarf luminosity function, augmented by white dwarfs in the LHS Eight Tenths Sample brighter than  $M_V = +13$ . Six white dwarfs in this diagram had tangential velocities in excess of  $v_{\text{tan}} = 250 \text{ km s}^{-1}$  that could be associated with the thick disk or halo populations. We reproduce in Figure 1 a similar result but for the white dwarf sample of Bergeron et al. (2001, hereafter BLR) composed of cool degenerates with trigonometric parallax and proper motion measurements, from which distances and thus tangential velocities can be determined. Note that  $M_B$  is used here instead of  $M_V$  in order to overplot the results of OHDHS discussed below. Five of the six halo white dwarf

candidates from Liebert et al. (1989) — LHS 56, LHS 147, LHS 282, LHS 291, and LHS 524 — are labeled in Figure 1; the missing object (LHS 2984) is below the range of the plot. We also marked three additional objects with large tangential velocities (G126–25, G138–56, and L845–70). The results displayed here indicate that most of these halo white dwarf candidates have parallax measurements with large uncertainties, however, which translate into large errors in both  $M_B$  and  $v_{\text{tan}}$ . Only LHS 56 and LHS 542 have errors smaller than 30%, while three objects have errors even larger than the measurement itself. The remaining white dwarfs in Figure 1 have estimated tangential velocities below  $\sim 175 \text{ km s}^{-1}$ , consistent with the disk population.

Also shown in Figure 1 are the results obtained for the 38 white dwarfs taken from Table 1 of OHDHS. The  $M_B$  values are derived from their photographic color-magnitude calibration,  $M_{B_J} = 12.73 + 2.58 (B_J - R_{59F})$ , and from the color equation of Blair & Gilmore (1982). As can be seen, a significant fraction of this sample stands out from the disk white dwarfs studied by BLR. This is actually the main argument used by OHDHS to interpret these high velocity stars as halo members. These results are discussed further in § 3 below.

We now proceed to analyze the optical *BVRI* and infrared *JHK* photometry (CCD) for the eight halo white dwarf candidates identified in Figure 1 (only three objects have infrared photometry available) using the model atmospheres and fitting technique described at length in Bergeron et al. (1997, hereafter BRL). Briefly, the optical and infrared magnitudes are first converted into average fluxes, which are then compared with those obtained from the model atmospheres — properly averaged over the filter bandpasses — using a nonlinear least-squares method. Only  $T_{\text{eff}}$  and the solid angle  $\pi(R/D)^2$  are considered free parameters. The distance  $D$  is obtained from the trigonometric parallax measurement, and the stellar radius  $R$  is converted into mass using the C/O-core evolutionary models described in Bergeron et al. (2001) with thin or thick hydrogen layers, which are based on the calculations of Fontaine et al. (2001). Note that a value of  $\log g = 8.0$  was assumed for four of these stars — LHS 282, G138–56, L845–70, and G126–25 — since their trigonometric parallax measurements are too uncertain to yield any meaningful value of the stellar radius and mass. Sample fits for the three white dwarfs with complete *BVRI* and *JHK* energy distributions are displayed in Figure 2, where both the monochromatic and average model fluxes are shown, although only the latter are used in the fitting procedure. High signal-to-noise spectroscopic observations at  $H\alpha$  (not shown here) confirm our solutions (see the discussion in BLR). We note already that the stars in Figure 2 have temperatures and masses that are quite similar to the  $\sim 150$  disk white dwarfs analyzed by BLR.

To estimate the age of these halo white dwarf candidates, we plot in the bottom panel of Figure 3 their location in a mass versus  $T_{\text{eff}}$  diagram together with the isochrones

from our C/O-core white dwarf cooling models with thick hydrogen layers; thin hydrogen layer models would yield ages that are  $\sim 1.5$  Gyr *younger*. Also shown are the corresponding isochrones but with the main sequence lifetime added to the white dwarf cooling age; here we simply assume (Leggett et al. 1998)  $t_{\text{MS}} = 10(M_{\text{MS}}/M_{\odot})^{-2.5}$  Gyr and  $M_{\text{MS}}/M_{\odot} = 8 \ln[(M_{\text{WD}}/M_{\odot})/0.4]$ . It is clear that none of these white dwarfs are old enough to be members of the galactic halo. On the contrary, they all lie comfortably within the bulk of other (young) disk white dwarfs taken from BLR, also displayed in the figure. Of course, several of the halo candidates selected from Figure 1 would have not been considered in the first place if the parallax measurement had been more accurate. But even LHS 56 ( $T_{\text{eff}} = 7270$  K) and LHS 542 ( $T_{\text{eff}} = 4720$  K, shown in Fig. 2), which have the best trigonometric parallax measurements, are about 2.0 and 8.5 Gyr old, respectively. This is considerably younger than what is expected from a stellar halo population, typically older than  $\sim 14$  Gyr.

These results, taken at face value, suggest that there exists a population of young white dwarfs, most likely formed in the thin disk, with large tangential velocities typical of the halo population ( $v_{\text{tan}} > 250$  km s $^{-1}$ ). The possible nature of these high velocity white dwarfs is discussed below in § 4. It also appears from our results that there are no white dwarfs with measured trigonometric parallaxes that are members of the galactic halo. Hence the luminosity function of halo white dwarfs determined by Liebert et al. (1989) and used by Chabrier et al. (1996) to estimate the white dwarf contribution to the halo missing mass is to be considered premature. With these results in mind, we now turn to the OHDHS sample.

### 3. White Dwarfs in the Oppenheimer et al. sample

#### 3.1. Reduced Proper Motion Diagram

We first begin by studying the reduced proper motion diagram, which is commonly used to identify halo white dwarf candidates in surveys based on digitized photographic plates (see, e.g., Knox et al. 1999; Hambly 2001, OHDHS). The reduced proper motion is defined as  $H_{\text{R}} = R_{59\text{F}} + 5 \log \mu + 5$ , where  $R_{59\text{F}}$  is the photographic magnitude, and  $\mu$  is the proper motion measured in arc seconds per year. As explained by Knox et al. (1999),  $H_{\text{R}}$  is an intrinsic property of the star that gives some estimate of its absolute magnitude. Stars that are relatively blue and with large values of  $H_{\text{R}}$  in this diagram are viewed as good halo white dwarf candidates since old, and thus cool, white dwarfs have low luminosities and turn blue below  $\sim 3500$  K (see Hambly 2001, for instance).

We show in Figure 4 the reduced proper motion diagram for the combined sample of

disk white dwarfs from BRL and BLR (note that trigonometric parallaxes are not required to construct this diagram) as well as the OHDHS sample. Since the OHDHS analysis relies on the photographic  $B_J - R_{59F}$  color index, the  $B$  and  $R$  magnitudes from BRL and BLR had to be converted into photographic magnitudes using the equations of Blair & Gilmore (1982) and Bessell (1986). There are two white dwarfs, LHS 147 and LHS 542, that are in common between the BRL/BLR and the OHDHS samples, and their location in Figure 4 are in excellent agreement. Five of the six halo white dwarf candidates identified by Liebert et al. (1989) and analyzed in the previous section are labeled in Figure 4. Obviously, these objects clearly stand out from the rest of the BRL and BLR samples of disk white dwarfs, but as shown above, this is mostly due to their large proper motions and not to their low luminosities. Their relatively blue color indices are representative of white dwarfs with effective temperatures well above 4000 K, and not indicative of extremely cool degenerates. So what we are seeing here is only a *vertical shift* with respect to the disk sequence.

The 38 white dwarfs from the OHDHS sample are displayed in Figure 4 as well (the different symbols are explained in § 4). We already note that about half of this sample overlaps completely with the disk population, and there is thus no indication, at least from this diagram, that this subsample should be associated with an older population of the Galaxy. Only the other half of the sample actually exhibits the required characteristics to be halo white dwarfs. It is interesting to note, however, that the candidates from Liebert et al. (1989) represent even more extreme cases than the OHDHS sample, yet none are halo members according to our detailed model atmosphere analysis.

The horizontal dotted line in Figure 4 delineates the region below which the Luyten catalogs contain very few objects according to OHDHS, primarily because Luyten’s survey in the Southern Hemisphere did not attempt to find objects as faint as those found by OHDHS. Interestingly enough, 10 out of the 13 white dwarfs from the BRL/BLR sample found below this limit are actually LHS stars. So with the exception of F351–50 and WD0351–564, the two reddest objects at the bottom of Figure 4, there is a considerable overlap in this diagram between these samples, despite the fact that OHDHS searched for objects as faint as  $R_{59F} = 19.8$ .

### 3.2. Color-Magnitude Diagrams

In order to estimate the tangential velocity of the white dwarfs in their sample, OHDHS relied on distances obtained from the photographic magnitudes  $B_J$  and their color-magnitude relation —  $M_{B_J} = 12.73 + 2.58 (B_J - R_{59F})$  — derived from a linear least-squares fit to the cool white dwarf sample of BLR. Figure 5 shows the  $M_{B_J}$  versus  $(B_J - R_{59F})$  color-magnitude

diagram for the BLR and OHDHS samples, together with the theoretical sequences obtained from model atmospheres with pure hydrogen and pure helium compositions. These models are similar to those described in BLR and references therein (see also Bergeron & Leggett 2002).

Of course, the OHDHS data all appear on the same line since their absolute magnitudes are based on a linear color-magnitude relation. Hence in their analysis, a given value of  $(B_J - R_{59F})$  yields a unique value of  $M_{B_J}$ , which combined with  $B_J$  gives the distance. The results displayed in Figure 5 indicate that their relation is indeed a pretty good match to the cool white dwarf sample of BLR, with the exception perhaps at the hot end of the sequence where a small but significant departure occurs. This could lead to distances being underestimated in this range of effective temperature. A similar conclusion was reached by Torres et al. (2002) who compared in their Figure 1 the OHDHS calibration with a Monte Carlo simulation of the disk white dwarf population (see comment below, however).

The main problem with this linear color-magnitude relation is that hydrogen-rich atmosphere white dwarfs do not become increasingly red as they cool off, but instead turn blue, as a result of the extremely strong collision-induced absorptions by molecular hydrogen (Hansen 1998; Saumon & Jacobson 1999; Bergeron & Leggett 2002). The effective temperature below which this phenomenon occurs depends of course on the color index considered. For instance, for a  $0.6 M_\odot$  white dwarf, the turnoff in  $(V - I)$  occurs at  $T_{\text{eff}} \sim 3500$  K, while for the  $(B_J - R_{59F})$  color index discussed here, it occurs near  $T_{\text{eff}} \sim 3000$  K. It is thus clear that the color-magnitude relation for hydrogen-rich atmosphere white dwarfs cannot be linear. The same conclusion applies to helium-rich atmosphere white dwarfs that contain only small traces of hydrogen, since such stars have energy distributions that are characterized by very strong infrared absorptions by molecular hydrogen resulting from collisions with neutral helium (Bergeron & Leggett 2002). Hence for a given value of  $(B_J - R_{59F})$ , or in general any color index in the visible region, there exist *two* possible values of the absolute magnitude for white dwarfs with atmospheres containing hydrogen.

Perhaps the best example is LHS 1402 whose spectrum is shown in Figure 2b of OHDHS, and which according to the authors is a cooler analog of LHS 3250 and SDSS 1337+00, re-analyzed recently by Bergeron & Leggett (2002). Its measured value of  $(B_J - R_{59F}) = 0.46$  implies an absolute magnitude of  $M_{B_J} = 13.92$ , or a distance of 76 pc ( $B_J = 18.32$ ), i.e. the value given in Table 1 of OHDHS. However, this would also imply according to Figure 5 that LHS 1402 has  $T_{\text{eff}} \sim 7000$  K, a temperature which can be completely ruled out according to the observed spectrum. If one assumes instead that LHS 1402 resides passed the turnoff on the pure hydrogen sequence shown in Figure 5, one derives instead  $M_{B_J} = 19.97$  (for  $M = 0.6 M_\odot$ ), or a distance of only 4.7 pc! LHS 1402 may thus be among the closest white dwarfs to

Earth. Of course, a full model atmosphere analysis of this object is required before reaching a firm distance estimate. The point remains that the linear color-magnitude relation used by OHDHS neglects the fact that there could be a substantial fraction of extremely cool white dwarfs in their sample, and that the distances to these objects may be largely overestimated. If this were true, the space density of halo white dwarfs derived by OHDHS could even be higher than the value they inferred.

### 3.3. Fits to the Energy Distributions

It has been argued by BRL and BLR that the best way to determine the fundamental parameters of cool white dwarf stars — effective temperature, mass, and atmospheric composition — is to use the entire energy distribution rather than to rely on the limited information contained in color-color or color-magnitude diagrams. This is particularly true if the  $B$  filter is used, since for hydrogen-rich atmosphere white dwarfs below  $T_{\text{eff}} \sim 5000$  K, there seems to be a missing source opacity in the ultraviolet unaccounted for in the model atmosphere calculations, resulting in an excess of flux in this particular region of the spectrum (see BRL, Bergeron 2001). This is the reason why in Figure 5, there appears to be a deficiency of  $\sim 0.6 M_{\odot}$  hydrogen-atmosphere white dwarfs below 5000 K, where all stars seem to follow instead the helium-atmosphere sequence. As shown in Figure 6, this discrepancy disappears if we consider a similar color-magnitude diagram for the BLR sample, but this time using  $M_R$  versus  $R - I$  in order to stay away from the ultraviolet regions. The location of the hydrogen-rich and helium-rich atmosphere white dwarfs in this diagram is consistent with the predicted colors.

It is worth mentioning here that the arguments presented by Torres et al. (2002) with respect to the color-magnitude calibration used by OHDHS, and in particular with the distances to the cool white dwarfs being overestimated, are not completely accurate. The calibration used by OHDHS has been determined empirically, and it is based on a least-squares fit to the white dwarf observations from BLR, as discussed above. In contrast, the Monte-Carlo simulations shown in Figure 1 of Torres et al. are based on *theoretical colors* taken from the cooling models of Salaris et al. (2000). Hence the magnitude discrepancy for the cool white dwarfs observed in their Figure 1 is simply the result of the missing source of opacity in the hydrogen model atmospheres from which the colors were calculated. Actually, the color-magnitude calibration of OHDHS yields more accurate distance estimates than the models, provided that the white dwarfs are hotter than  $\sim 3500$  K. Similarly, the conclusions of Torres et al. regarding the objects lying beyond the turn-off in Figure 5 as being necessarily helium-atmosphere white dwarfs is also misleading since these stars could

as well have hydrogen atmospheres if one considers the more appropriate  $M_R$  versus  $R - I$  diagram displayed in Figure 6. Such ambiguities can be easily avoided by taking into account the complete energy distributions.

Ideally, energy distributions should be built from optical  $BVRI$  and infrared  $JHK$  photometric measurements, but such measurements are not available for the moment for the OHDHS sample. Nevertheless, we can get some insight into the nature of these white dwarfs by using the photographic  $BRI$  magnitudes published by OHDHS. We thus proceed with fitting these white dwarfs by first transforming the photographic magnitudes into standard  $BRI$  magnitudes using the equations of Blair & Gilmore (1982) and Bessell (1986), as well as the empirical relation  $(B - V) = 0.097 + 0.612 (R - I) + 2.136 (R - I)^2$  derived from the BRL and BLR observations. These magnitudes are then converted into broadband fluxes and compared with the predictions of our model atmospheres using the fitting technique described in § 2. Since there is no trigonometric parallax measurement for these stars, a value of  $\log g = 8.0$  is assumed for all objects.

With the lack of infrared measurements, it may be difficult to determine whether a cool white dwarf has a hydrogen- or helium-rich atmosphere. For stars above  $T_{\text{eff}} \sim 5000$  K, however, BRL have shown that the presence of  $H\alpha$  implies in general that the white dwarf has a hydrogen-rich atmosphere, while the absence of this feature implies a helium-rich atmosphere. We have thus used the spectroscopic information available in Table 1 of OHDHS to establish the atmospheric composition of all stars above  $T_{\text{eff}} = 5000$  K. This was possible for 20 out of 38 white dwarfs in the sample. Typical fits are displayed in Figure 7 for hydrogen and helium atmosphere white dwarfs. Predicted broadband fluxes are shown at  $BVRI$  as well as  $JHK$ . For stars below 5000 K, it is not possible to determine the atmospheric composition unambiguously, as shown for the two objects at the bottom of Figure 7. Clearly, infrared measurements would help to discriminate between the two solutions. The atmospheric composition can nevertheless be inferred for two cool white dwarfs in the sample: LHS 542, which has been analyzed by BLR, has a complete energy distribution consistent with a helium-rich atmosphere (see Fig. 2). Also, the spectrum of LHS 1402 displayed in Figure 2 of OHDHS reveals a very strong near infrared flux deficiency, suggesting a hydrogen-rich composition. We are thus left with 16 out of 38 stars with no information about the atmospheric composition.

The problem becomes even more complex when one considers the results shown in Figure 5, which reveal that for some cool stars, three solutions are possible: a cool helium atmosphere, a cool ( $T_{\text{eff}} \lesssim 3000$  K) or a hot ( $T_{\text{eff}} \gtrsim 3000$  K) hydrogen atmosphere. In the absence of infrared photometric measurements, it is difficult to distinguish between these three solutions. In addition, because of the missing source of UV opacity in the

hydrogen model atmospheres (see discussion above), it may even be dangerous to rely on the  $B$  magnitudes for these cool white dwarfs. We have thus followed the prescription of BLR and omitted the  $B$  filter when fitting the coolest white dwarfs in the sample with pure hydrogen models. Our fitting procedure is illustrated in Figure 8 for the reddest objects in the color-magnitude diagram shown in Figure 5. F351–50 and WD0205–053 are so red that a unique hydrogen solution is found, which corresponds to the hydrogen model that produces the reddest possible value of  $(R - I)$ ; the bad resulting fit suggests that these stars probably have helium-rich atmospheres instead. WD0351–564 and WD0345–362 on the other hand have two possible hydrogen solutions that differ only by the quality of the fit at  $B$ . The large discrepancy observed at  $B$  for the warm hydrogen solutions suggest that the cool solutions are probably more appropriate. Again, it is obvious that infrared photometric observations would help to constrain the solutions better. For the time being, however, we will retain what appears to be the “best” hydrogen solution, as well as the helium solution, for all cool white dwarfs in the sample.

To summarize our results, all white dwarfs with  $T_{\text{eff}} > 5000$  K have effective temperatures and atmospheric compositions that are well constrained by our fitting technique, while cooler stars possess at least two possible solutions that depend on the assumed atmospheric composition, but both solutions are nevertheless below 5000 K.

The accuracy of our fitting procedure using the limited information contained in the energy distributions based solely on  $BRI$  can be assessed by comparing the effective temperatures of the two white dwarfs in common between the OHDHS and the BLR samples for which we have complete energy distributions. For LHS 147, we obtain  $T_{\text{eff}} = 7310$  K from  $BRI$  alone, which can be compared with  $T_{\text{eff}} = 7600$  K when the complete energy distribution is used (see Fig. 2), whereas for LHS 542 we derive  $T_{\text{eff}} = 4780$  K versus 4720 K under similar conditions. This comparison indicates that the temperature scale obtained here is quite reliable for the purpose of our discussion.

#### 4. Results and Discussion

The effective temperature distribution of the halo white dwarf candidates in the OHDHS sample is displayed as a histogram in the top panel of Figure 3, with the number of stars in each 1000 K bin shown on the left hand side of the figure. For the cooler stars, we have taken the average of the hydrogen and helium atmosphere solutions; there is also one star, LP 586–51, with a temperature of  $\sim 14,000$  K outside the range of the plot. About 75% of the stars in the OHDHS sample have effective temperatures above 4000 K, and unless their masses are very close to  $0.45 M_{\odot}$ , they are obviously too young to be associated with the halo

population. Even though the halo membership of these stars cannot be completely ruled out until precise trigonometric parallax measurements are secured, it seems more reasonable, in the light of the results obtained for the halo white dwarf candidates identified by Liebert et al. (1989), also shown in Figure 3, to associate these OHDHS stars with the same population of young, high velocity white dwarfs.

We note also in Figure 3 that all seven stars in the 3000-4000 K bin have effective temperatures taken as the average of the hydrogen and helium atmosphere solutions below and above  $T_{\text{eff}} = 4000$  K, respectively. If infrared measurements confirm that these stars have helium atmospheres, this particular bin could end up empty! Also, the object in the coolest bin corresponds to LHS 1402, the white dwarf with the strong infrared flux deficiency discussed above. As demonstrated by Bergeron & Leggett (2002), if this flux deficiency is the result of collision-induced absorptions by molecular hydrogen due to collisions with *neutral helium* in a helium-rich atmosphere, rather than with other hydrogen molecules in a hydrogen-rich atmosphere, the effective temperature derived here from pure hydrogen models could be significantly underestimated. This would leave no ultracool, and presumably old, white dwarfs in the OHDHS sample.

Probably the most puzzling result of our analysis is illustrated in Figure 4 where white dwarfs with  $T_{\text{eff}} > 5000$  K are shown as filled diamonds, while cooler stars are indicated by filled circles. These results reveal that the hottest stars in the OHDHS sample correspond to the objects that lie below the sequence defined by the disk white dwarfs, with only a few cooler white dwarfs found in the same region of the diagram. The object at  $H_R = 21.3$  and  $(B_J - R_{59F}) = 0.46$  is LHS 1402, the coolest white dwarf in the sample; there is also LHS 542, labeled in the figure, which we know is too young to be a halo white dwarf. With the additional exception of F351–50 and WD0351–564 at the bottom of the diagram, all white dwarfs with  $T_{\text{eff}} < 5000$  K in the OHDHS sample overlap comfortably with the disk white dwarfs analyzed by BRL and BLR. There is thus no reason left to believe that even the cool stars in the OHDHS sample belong to an old galactic population, either from kinematics or age considerations. We are thus forced to conclude that white dwarfs identified in such reduced proper motion diagrams, and interpreted as halo candidates, should rather be associated with a hotter and presumably younger population of the Galaxy. We note that LHS 1402, probably the most promising halo candidate in the OHDHS sample, does not even particularly stand out in this reduced proper motion diagram.

It is interesting to mention in this context that Hambly (2001) has identified three halo white dwarf candidates from such a reduced proper motion diagram (see his Figure 1). His most extreme case (point indicated by a circle in his diagram) has a large reduced proper motion and relatively blue color, which make this object a very good halo candidate according

to Hambly. However, from the published *BRI* colors, we derive an effective temperature of  $\sim 7200$  K for this star using our fitting procedure, which suggests that this object also belongs to the same population of young high velocity white dwarfs found in the Liebert et al. (1989) and OHDHS samples.

Similar conclusions can be reached if we consider once again the distribution of tangential velocities with  $M_B$ , shown in Figure 9, but this time using our own distance estimates for the calculations of  $v_{\text{tan}}$ . As can be seen, all white dwarfs in the OHDHS sample with  $M_B \lesssim 15$  have high tangential velocities characteristic of the halo population. Yet, according to our  $T_{\text{eff}}$  determinations, these are probably too hot and too young to belong to the halo population. For  $M_B \gtrsim 15$ , the location of all white dwarfs in the OHDHS sample is consistent with the disk population, with the exception of LHS 542, F351–50, and WD0351–564. As mentioned above, LHS 542 is certainly too young to be a halo member. At the top of this diagram lies LHS 1402, with a tangential velocity entirely consistent with the disk population. Hence, even if this star stands out marginally in the reduced proper motion diagram shown in Figure 4, its tangential velocity is too small to be associated with the halo. We note that LHS 1402 could be made much more luminous ( $M_B \sim 16$ ) if it has a helium-dominated atmosphere similar to those of LHS 3250 and SDSS 1337+00 (see Fig. 8 of Bergeron & Leggett 2002). We are thus left with only two objects in the OHDHS sample, F351–50 and WD0351–564, that have the expected properties of halo white dwarfs, that is high tangential velocities and low effective temperatures, and even those could represent the cooled down version of the young high velocity white dwarf population unveiled here.

To summarize our findings, the OHDHS sample seems to be composed of two distinct white dwarf components. The first one – about half of the sample – is composed of cool white dwarfs which clearly belong to the disk population, as there are no indication that any of these stars differ from the other disk white dwarfs analyzed by BRL and BLR. The second component is composed of relatively warm white dwarfs with peculiarly high tangential velocities. Unless these white dwarfs all have masses close to  $0.45 M_{\odot}$ , they are too young to be associated with the halo population, or even with the thick disk. One argument in favor of these stars having normal masses ( $M \sim 0.6 M_{\odot}$ ) and being relatively young is provided by the analysis of the high velocity LHS stars with measured parallaxes, for which mass estimates indicate ages much lower than 10 Gyr (see Figures 2 and 3). If this interpretation is correct, they were probably born in the disk of the Galaxy, and somehow were accelerated by some mechanism.

One such possible mechanism has been explored quantitatively by Hansen (2002) who proposed that these high velocity white dwarfs are the remnants of donor stars from close mass-transfer binaries that produced type Ia supernovae via the single degenerate channel.

As the close binary orbit gets disrupted by the supernova explosion, the donor star is simply released, and eventually evolves to the white dwarf stage with its pre-supernova high orbital velocity. Hansen argues that the local density of such high velocity remnants is comparable to that determined by OHDHS for their sample. One consequence of this proposed scenario is that none of these white dwarfs could have a binary companion. This seems at least consistent with our results for the high velocity LHS stars, as none of them appear to be overluminous (i.e. they are consistent with being single stars). Other alternative mechanisms have been proposed by Davies et al. (2002) and Koopmans & Blandford (2002) by which stars can be ejected from the thin disk into the galactic halo with the required high velocities.

Further progress in answering some of the issues raised in this paper can be achieved with the help of high quality *BVRI* and *JHK* photometric observations for the coolest stars in the OHDHS sample. Trigonometric parallax measurements would also be required to measure the individual white dwarf masses and obtain more accurate estimates of the stellar ages. Such an endeavor is currently underway.

This work was supported in part by the NSERC Canada and by the Fund NATEQ (Québec).

## REFERENCES

- Bergeron, P. 2001, *ApJ*, 558, 369
- Bergeron, P., & Leggett, S. K. 2002, *ApJ*, in press
- Bergeron, P., Leggett, S. K., & Ruiz, M. T. 2001, *ApJS*, 133, 413 (BLR)
- Bergeron, P., Ruiz, M. T., & Leggett, S. K. 1997, *ApJS*, 108, 339 (BRL)
- Bessell, M. S. 1986, *PASP*, 98, 1303
- Blair, M., & Gilmore, G. 1982, *PASP*, 94, 742
- Chabrier, G., Segretain, L., & Méra 1996, *ApJ*, 468, L21
- Davies, M. B., King, A., & Ritter, H. 2002, *MNRAS*, 333, 463
- Fontaine, G., Brassard, P., & Bergeron, P. 2001, *PASP*, 113, 409
- Hambly, N. C. 2001, in *ASP Conf. Ser. Vol. 226, 12th European Workshop on White Dwarf Stars*, eds. J. L. Provençal, H. L. Shipman, J. MacDonald, & S. Goodchild, 381
- Hansen, B. M. S. 1998, *Nature*, 394, 860
- Hansen, B. M. S. 2001, *ApJ*, 558, L39
- Hansen, B. M. S. 2001, *ApJ*, in press
- Knox, R. A., Hawkins, M. R. S., & Hambly, N. C. 1999, *A&A*, 306, 736
- Koopmans, L. V. E., & Blandford, R. D. 2002, preprint (astro-ph/0107358)
- Leggett, S. K., Ruiz, M. T., & Bergeron, P. 1998, *ApJ*, 497, 294
- Liebert, J., Dahn, C. C., & Monet, D. G. 1988, *ApJ*, 332, 891
- Liebert, J., Dahn, C. C., & Monet, D. G. 1989, in *IAU Colloq. 114, White Dwarfs*, ed. G. Wegner (Berlin: Springer), 15
- Oppenheimer, B. R., Hambly, N. C., Digby, A. P., Hodgkin, S. T., & Saumon, D. 2001, *Science*, 292, 698 (OHDHS)
- Reid, I. N., Sahu, K. C., & Hawley, S. L. 2001, *ApJ*, 559, 942
- Salaris, M., García-Berro, E., Hernanz, M., Isern, J., & Saumon, D. 2000, *ApJ*, 544, 1036

Saumon, D., & Jacobson, S. B. 1999, ApJ, 511, L107

Torres, S., García-Berro, E., Burkert, A., & Isern, J., 2002, MNRAS, 336, 971

Fig. 1.— Distribution of tangential velocities ( $v_{\text{tan}}$ ) with the  $B$  absolute magnitudes ( $M_B$ ) for all cool ( $T_{\text{eff}} < 12,000$  K) white dwarfs with trigonometric parallax measurements (*filled circles*), and for the halo white dwarf candidates taken from Table 1 of OHDHS (*open circles*). The white dwarfs with known distances that have tangential velocities consistent with a halo population are labeled in the Figure, and the associated uncertainties are shown as well.

Fig. 2.— Fits to the energy distributions of three halo white dwarf candidates with pure hydrogen atmosphere (*filled circles*) or pure helium atmosphere (*open circles*) models. The optical  $BVRI$  and infrared  $JHK$  photometric observations are shown by the error bars. The solid lines correspond to the model monochromatic fluxes, while the filled or open circles represent the average over the filter bandpasses. For LHS 282, a value of  $\log g = 8.0$  was assumed.

Fig. 3.— Top panel: Masses of white dwarfs in the trigonometric parallax sample of BLR (*open circles*), and halo white dwarf candidates (*filled symbols*; filled squares indicate stars for which  $\log g = 8.0$  was assumed) as a function of effective temperature, together with the isochrones from cooling sequences with C/O-core,  $q(\text{He}) \equiv M_{\text{He}}/M_{\star} = 10^{-2}$ , and  $q(\text{H}) = 10^{-4}$  (*solid lines*). The isochrones are labeled in units of  $10^9$  years. Also shown are the corresponding isochrones with the main sequence lifetime taken into account (*dotted lines*). Bottom panel: This histogram will be discussed in § 4.

Fig. 4.— Reduced proper motion diagram for the OHDHS sample (*filled symbols*; the distinction between the filled circles and filled diamonds is explained in § 4) and the combined BRL and BLR samples (*open circles*). The objects labeled correspond to the halo white dwarf candidates identified by Liebert et al. (1989), and analyzed in § 2. LHS 147 and LHS 542 are in common between the OHDHS and BRL samples, and their individual measurements are connected by dotted lines. The horizontal dotted line delineates the region below which the Luyten catalogs contain very few objects according to OHDHS. The two reddest white dwarfs at the bottom of the diagram are F351–50 and WD0351–564.

Fig. 5.—  $M_{B_J}$  vs.  $(B_J - R_{59F})$  color-magnitude diagram for the cool white dwarfs from BLR with measured trigonometric parallaxes, together with the linear relation used by OHDHS to estimate the absolute magnitudes for the stars in their sample from the  $(B_J - R_{59F})$  photographic color indices. Also shown are the theoretical colors for the pure hydrogen (*solid line*) and pure helium (*dotted line*) model atmospheres with, from top to bottom,  $M = 0.4, 0.6, 0.8, 1.0,$  and  $1.2 M_{\odot}$ . Effective temperatures are indicated in units of  $10^3$  K.

Fig. 6.—  $M_R$  vs.  $(R - I)$  color-magnitude diagram for the cool white dwarfs from BLR with hydrogen- (*solid dots*) and helium-rich (*open circles*) atmospheres. Also shown are the theoretical colors for the pure hydrogen (*solid line*) and pure helium (*dotted line*) model

atmospheres with, from top to bottom,  $M = 0.4, 0.6, 0.8, 1.0,$  and  $1.2 M_{\odot}$ . Effective temperatures are indicated in units of  $10^3$  K.

Fig. 7.— Typical fits to the energy distributions of halo white dwarf candidates from OHDHS with pure hydrogen atmosphere (*filled circles*) or pure helium atmosphere (*open circles*) models. The optical *BRI* photometric observations are shown by the error bars, while the filled or open circles represent the predicted model broadband fluxes et *BVRIJHK*. A value of  $\log g = 8.0$  was assumed for all objects. Two solutions are possible for the coolest white dwarfs shown at the bottom.

Fig. 8.— Same as Figure 7 but for the reddest objects shown in Figure 5. Note that the *B* magnitude is not used for the fits with pure hydrogen models (*filled symbols*). Some objects have also two possible hydrogen solutions.

Fig. 9.— Distribution of tangential velocities ( $v_{\text{tan}}$ ) with the *B* absolute magnitudes ( $M_B$ ) for the white dwarfs of OHDHS with  $T_{\text{eff}} > 5000$  K (*filled diamonds*) and  $T_{\text{eff}} < 5000$  K (*filled circles*). The trigonometric parallax sample of BLR shown in Figure 1 is reproduced here as well (*open circles*).

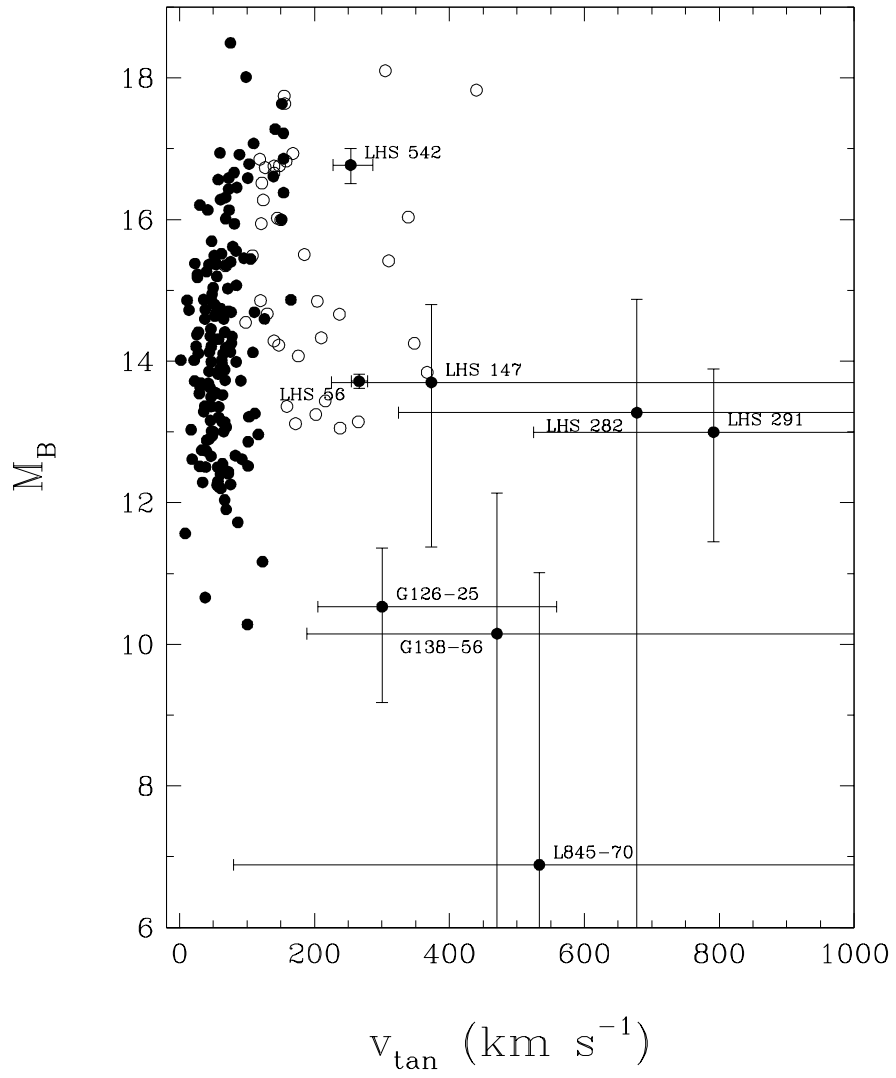


Figure 1

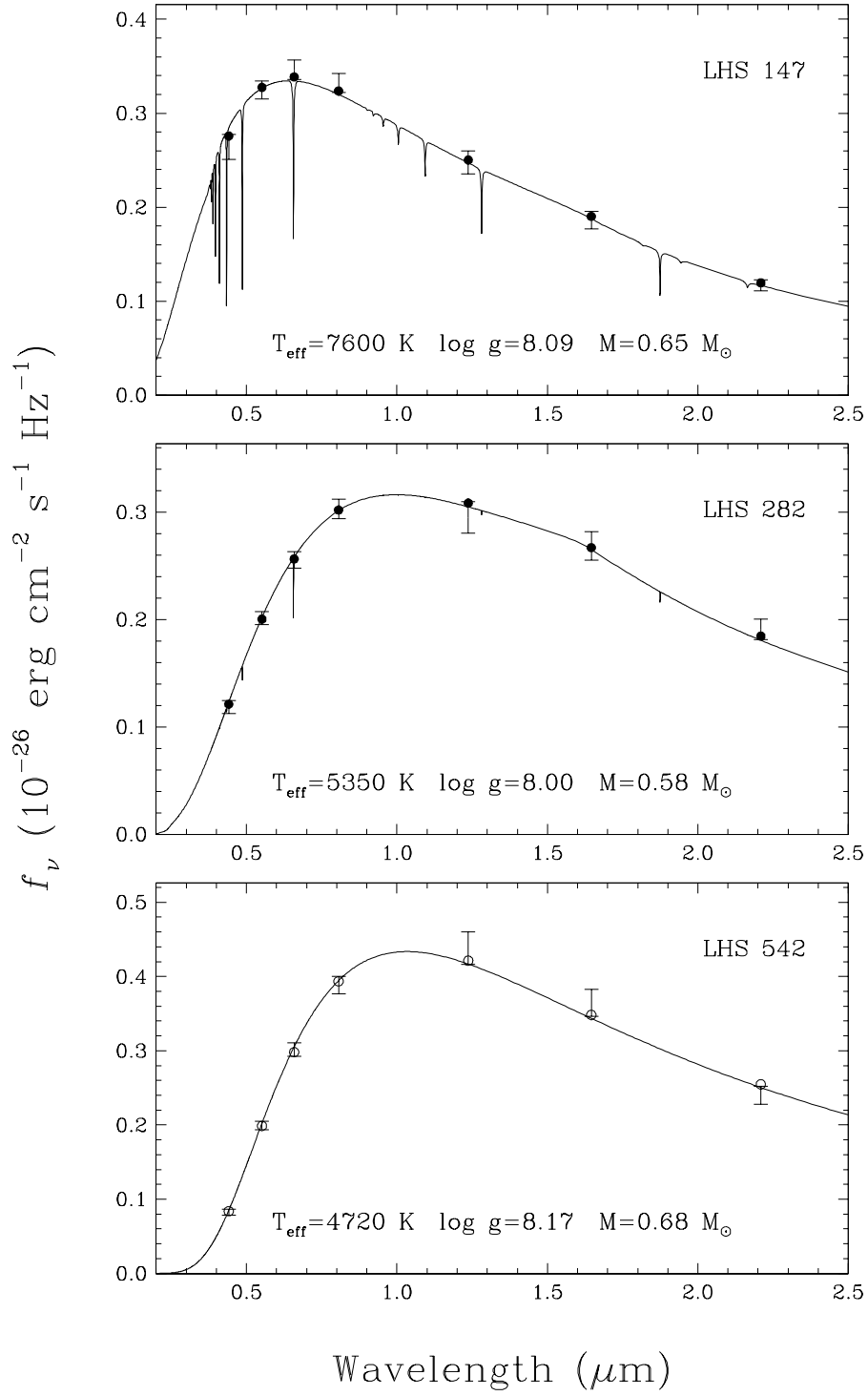


Figure 2

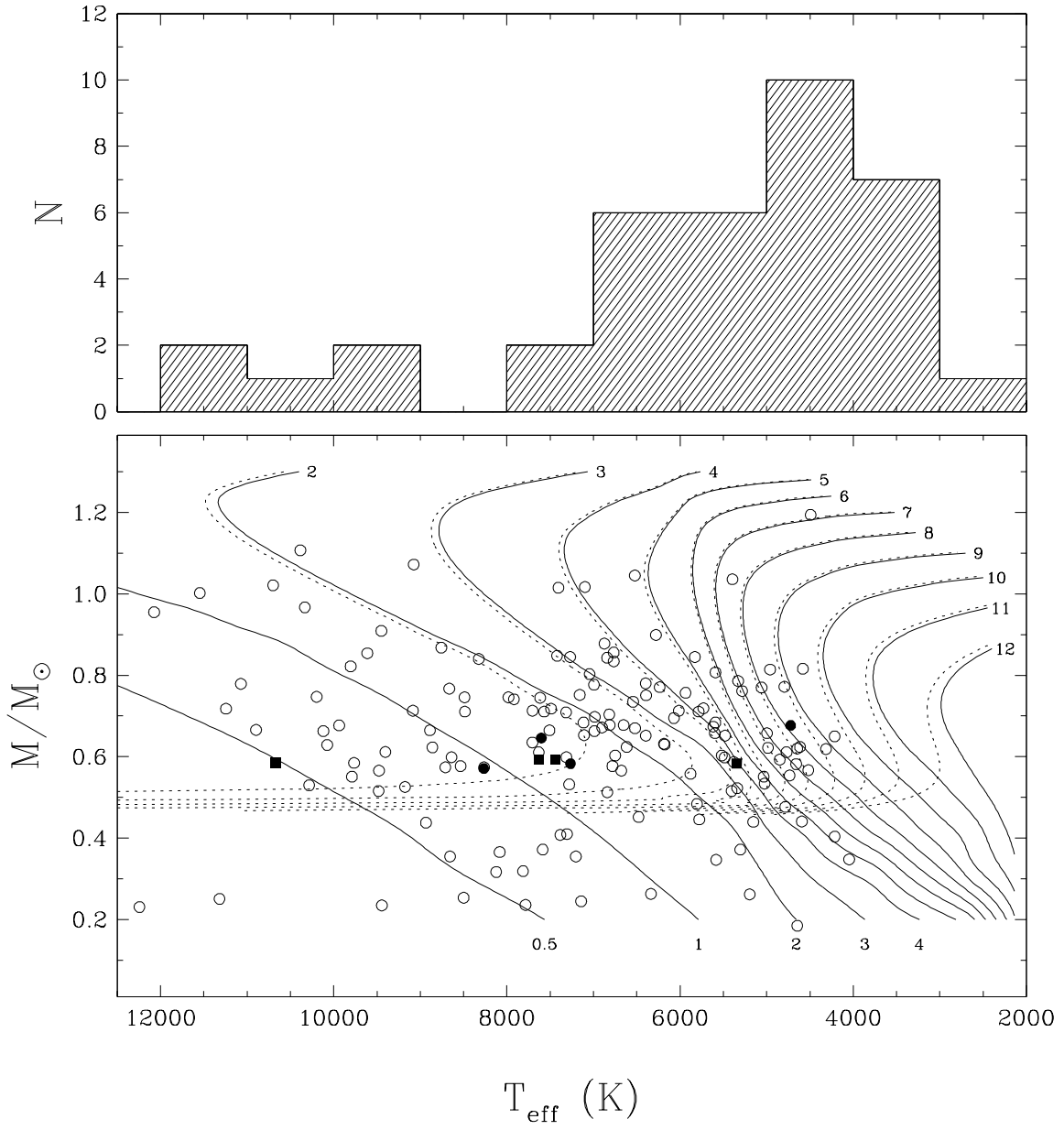


Figure 3

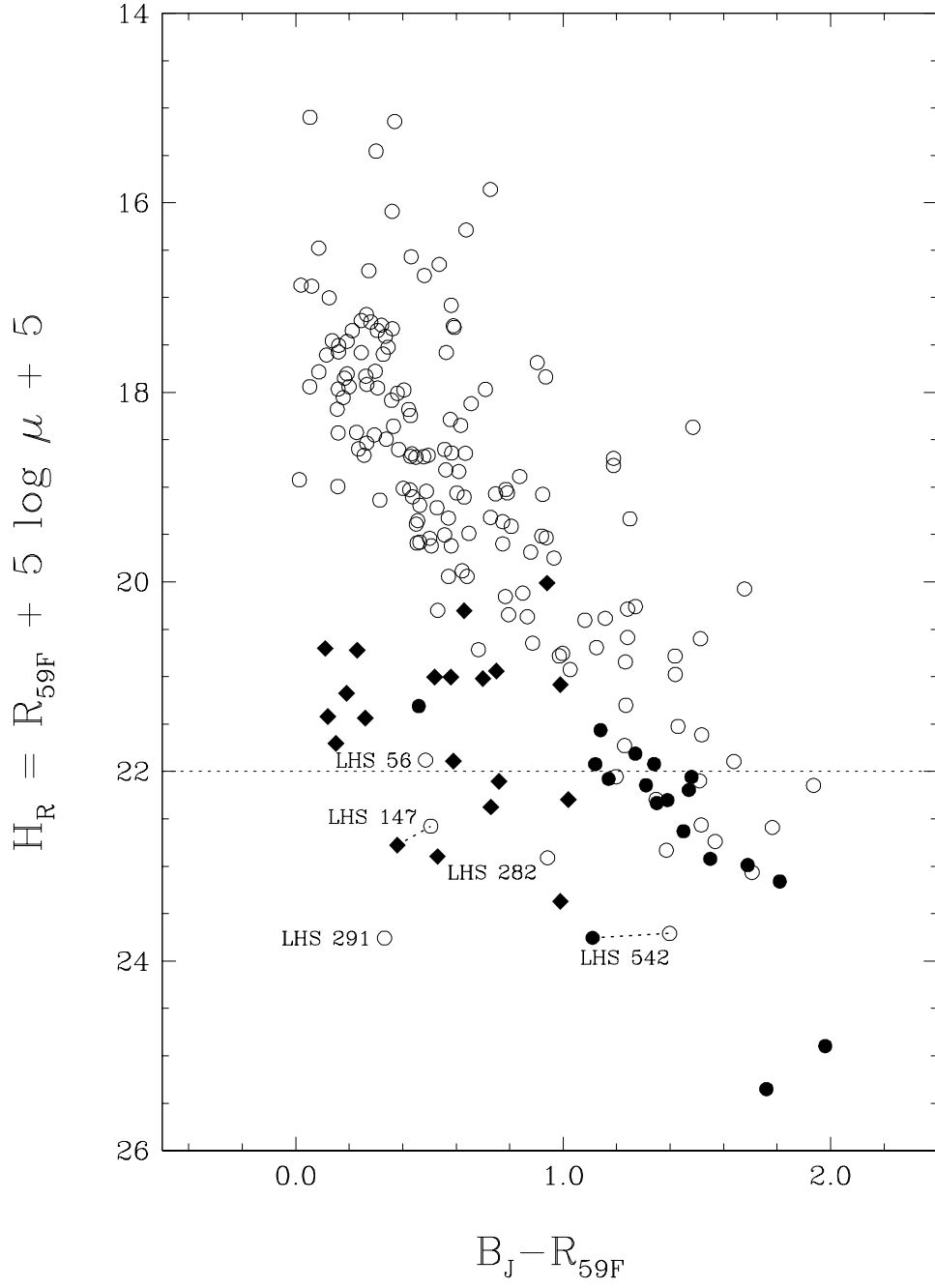


Figure 4

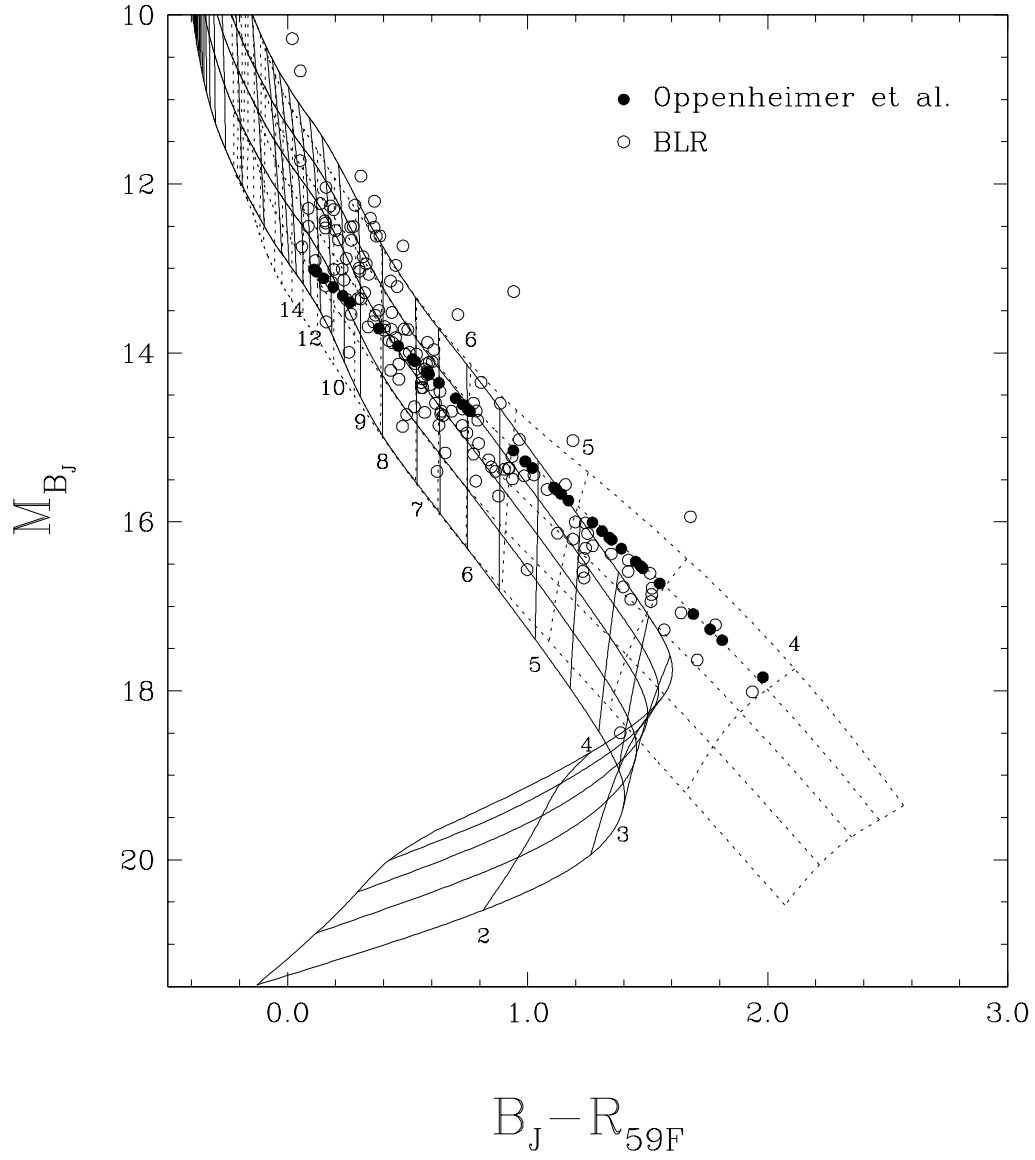


Figure 5

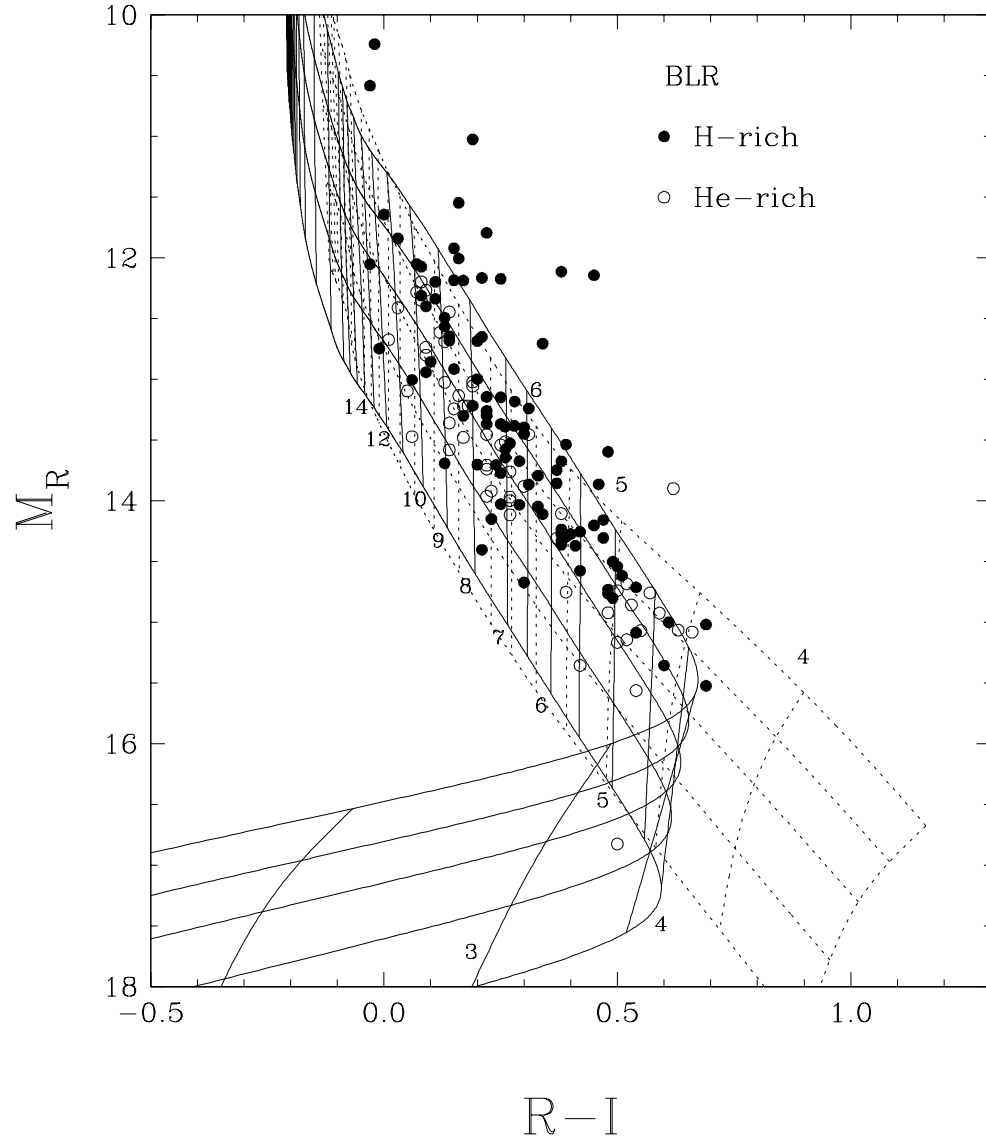


Figure 6

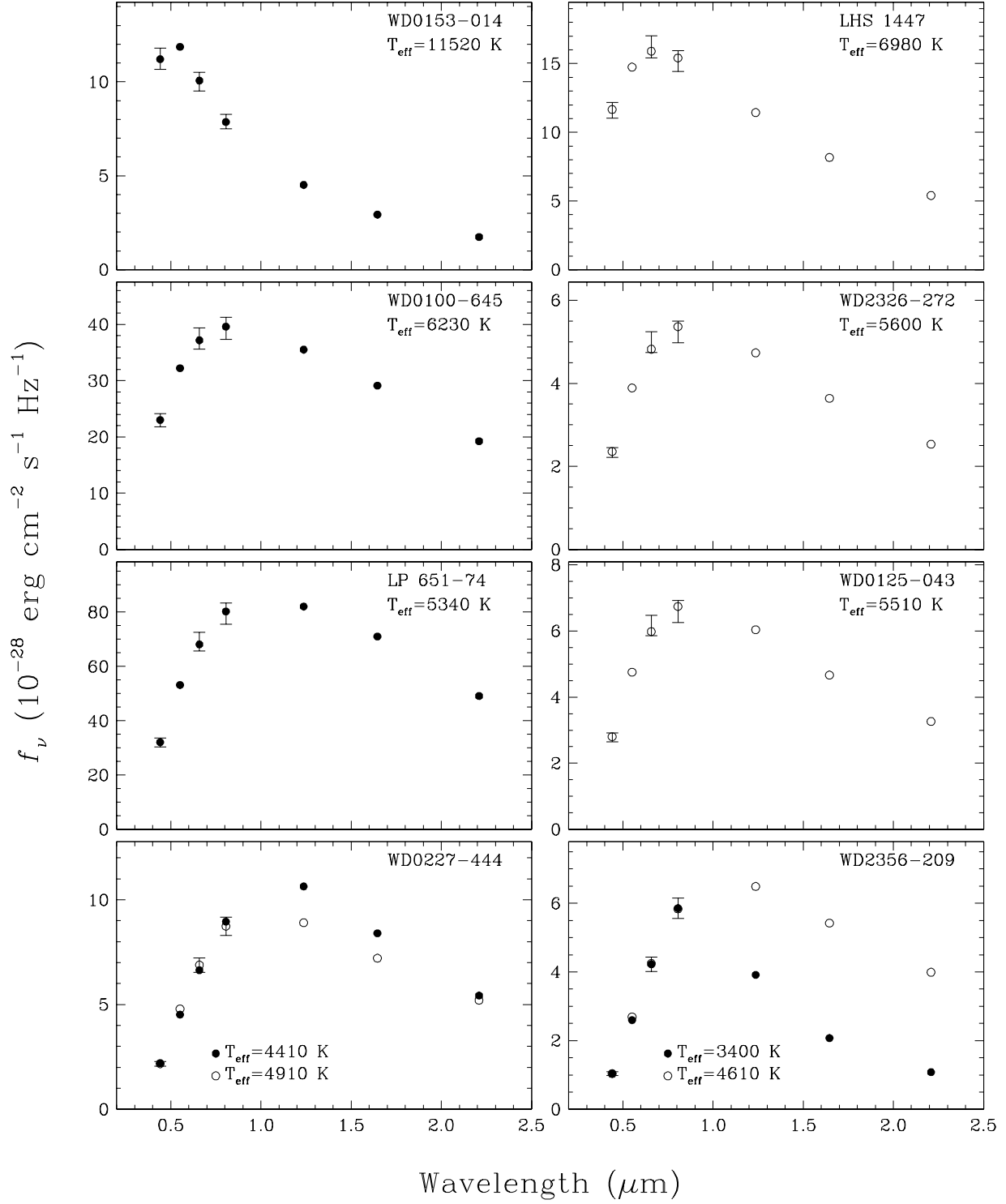


Figure 7

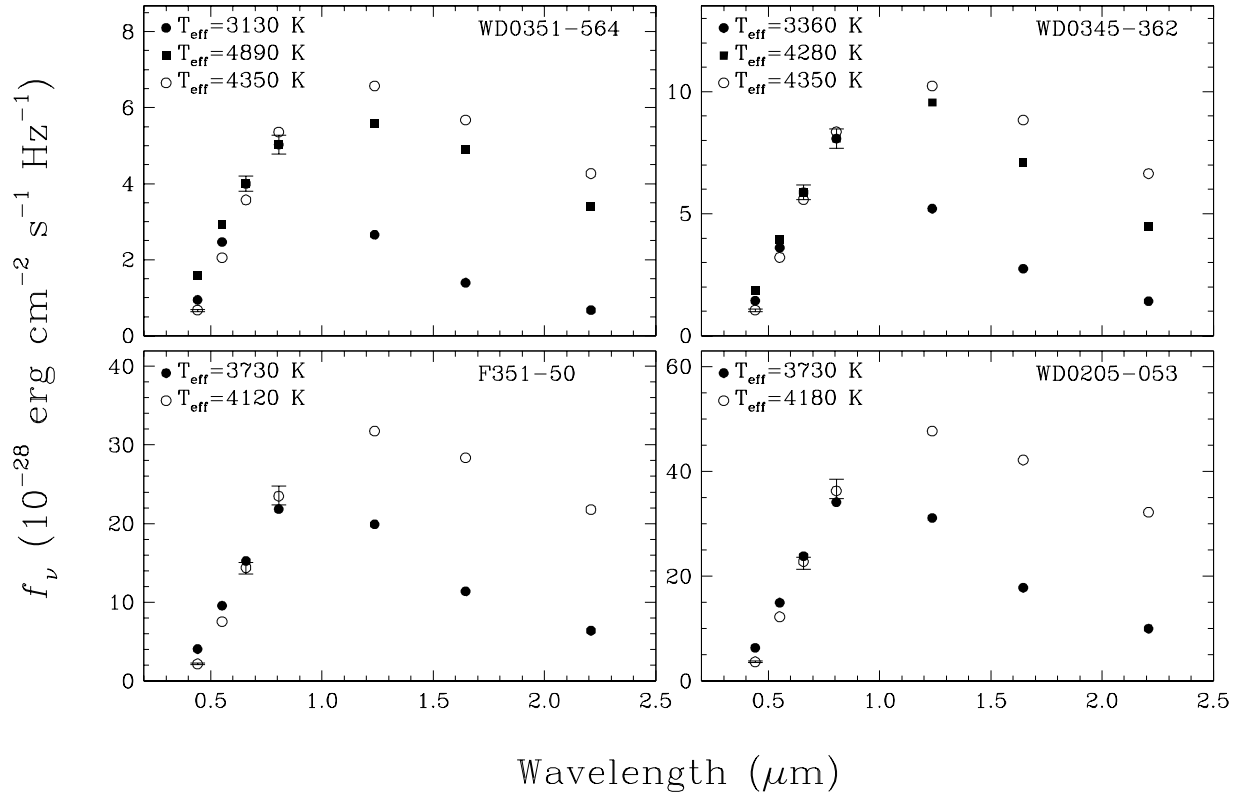


Figure 8

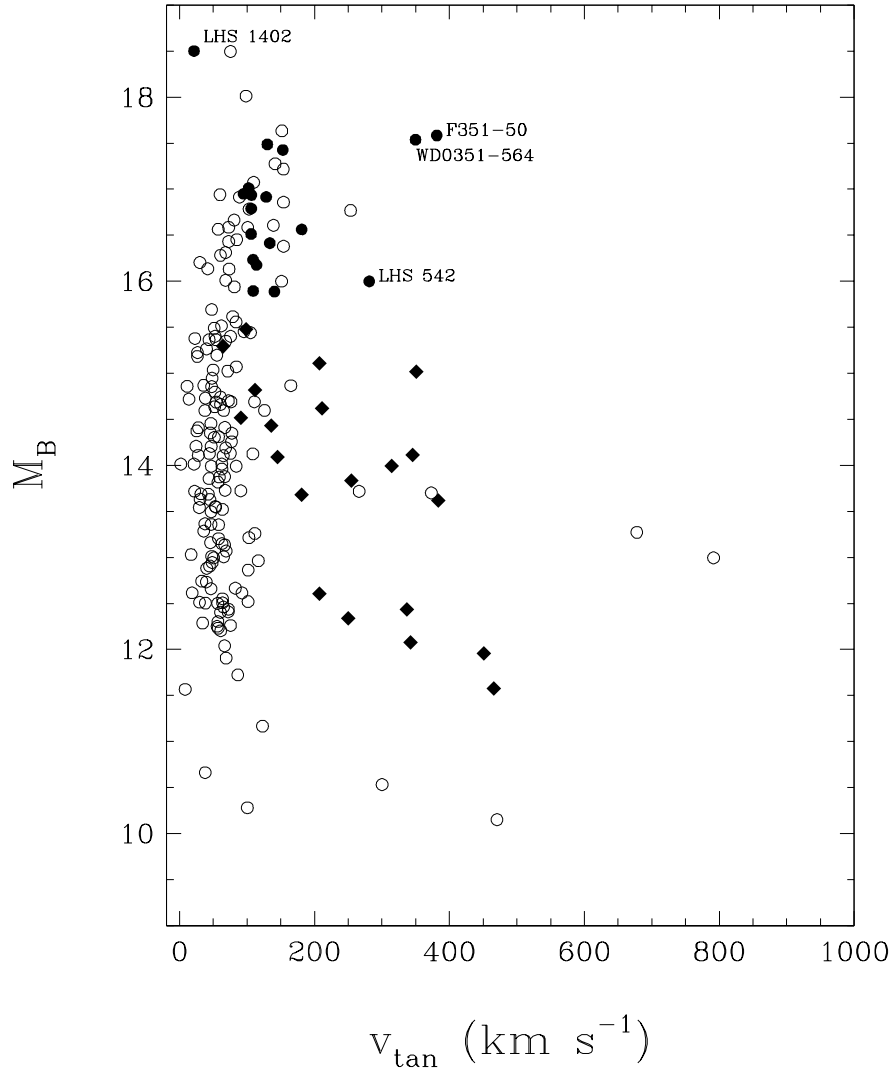


Figure 9